

## Four-wave mixing in alexandrite crystals

Ali M. Ghazzawi, Jacek K. Tyminski, and Richard C. Powell  
*Physics Department, Oklahoma State University, Stillwater, Oklahoma 74078*

John C. Walling  
*Allied Chemical Corporation, Mt. Bethel, New Jersey 07060*  
 (Received 30 July 1984)

Degenerate four-wave mixing was observed in alexandrite crystals ( $\text{BeAl}_2\text{O}_4:\text{Cr}^{3+}$ ), and the signal beam efficiency and decay rate were measured as functions of pump beam-crossing angle, wavelength, and power. The results are consistent with scattering from excited-state population gratings related to the difference in dispersion of the  $\text{Cr}^{3+}$  ions in the ground and metastable states. These gratings can be selectively established with  $\text{Cr}^{3+}$  ions in the inversion or mirror sites depending on the excitation wavelength. Strong scattering occurs only for pump beams polarized parallel to the  $b$  direction of the crystal.

### I. INTRODUCTION

The most successful type of tunable solid-state laser developed to date is based on alexandrite crystals ( $\text{BeAl}_2\text{O}_4:\text{Cr}^{3+}$ ).<sup>1</sup> Because of this, there has been a significant amount of work done in studying the properties of alexandrite.<sup>2-9</sup> One area that has not yet been thoroughly investigated is the nonlinear optical characteristics of this material. Such characteristics can be important in determining device properties for high-power laser operation. One manifestation of nonlinear interactions of laser beams in a solid is four-wave mixing (FWM) which occurs through the third-order component of the susceptibility tensor. FWM can arise from several different types of physical processes including thermal, excited-state population, and charge-migration effects. It has practical applications in optical information processing and phase conjugation,<sup>10</sup> as well as being a useful spectroscopic tool for studying properties of solids which are difficult to investigate by other methods.<sup>11</sup> We report here the first measurements of four-wave mixing in alexandrite crystals and show that the results are consistent with a model based on excited-state population gratings of  $\text{Cr}^{3+}$  ions in different types of sites.

The sample investigated was an oriented cube of  $\text{BeAl}_2\text{O}_4$  with each edge measuring about 5 mm. It contained 0.0897 at. %  $\text{Cr}^{3+}$  ions with about 78% of these being in mirror sites and the rest in inversion sites. The experimental setup used for degenerate four-wave mixing measurements was described previously<sup>11</sup> and is shown schematically in Fig. 1. The work discussed here was done at room temperature using either an argon-ion laser or a ring dye laser with R6G dye as a source. The powers of the write beams ( $P_1, P_2$ ) and the read beam ( $P_r$ ) are controlled by the variable beam splitter and neutral-density filter (VBS, VND). The write beams cross in the sample at an angle  $\theta$  and their interference forms a sine-wave pattern which acts as an index of refraction grating. A chopper (CH) is used to turn off the write beams. The read beam enters the sample in a direction phase conju-

gate to the write beam  $P_1$  and is partially diffracted by the grating. The Bragg diffraction condition results in the signal beam leaving the sample in a direction phase conjugate to write beam  $P_2$ . The intensity and decay time of the signal beam are related to the modulation depth and relaxation of the grating.

### II. SUMMARY OF RESULTS

Attempts were made to perform the experiments with all combinations of crystal orientations and laser polarizations. Strong FWM signals were only observed with laser beams polarized parallel to the  $b$  axis with propagation occurring along either of the other two crystallographic directions as shown in Fig. 2. Much weaker signals were obtained for light polarized parallel to the  $c$  axis and no FWM signal could be detected for light polarized parallel to the  $a$  axis. Figures 3 and 4 summarize the observed FWM characteristics obtained with the strong signal geometry shown in Fig. 2.

Degenerate FWM measurements were made for three laser wavelengths, 488.0, 514.5, and 579.1 nm. The signal

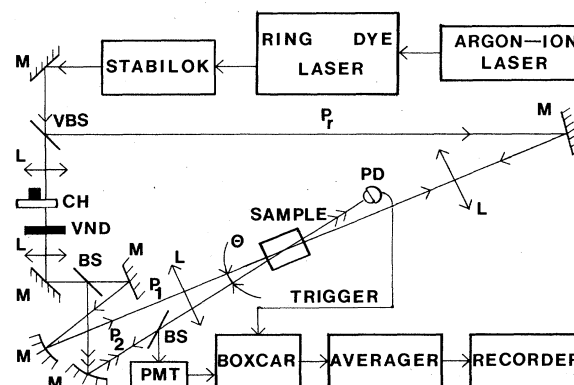


FIG. 1. Block diagram of experimental apparatus used for four-wave mixing.

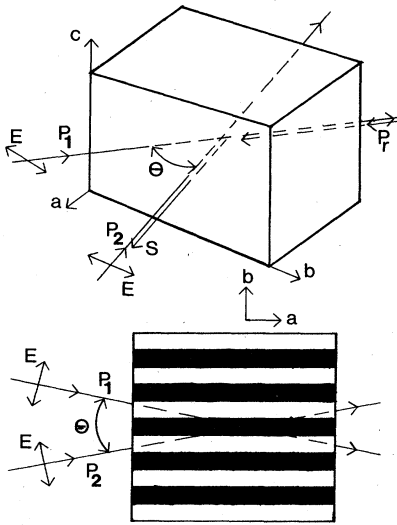


FIG. 2. Geometry of the laser-beam directions and polarizations with respect to the crystallographic axes for obtaining a strong FWM signal in alexandrite crystals.

beam decay rate  $K$  and scattering efficiency  $\eta$ , were determined at various write-beam crossing angles between  $1.75^\circ$  and  $26.5^\circ$  with various laser powers between about 2 and 400 mW for each write beam. The signal decay was purely exponential for all measurements in the time regime investigated. The decay rate was found to be independent of pump beam crossing angle  $\theta$  for all three wavelengths as shown in Fig. 3(a). The magnitude of the decay rate was significantly different for long wavelength pumping compared to pumping with the two shorter wavelengths. For each case it was approximately equal to twice the fluorescence decay rate shown as solid points at  $\theta=0^\circ$ . The grating decay rates were also found to be independent of the power in the write beams as shown in Fig. 3(b).

For the long-wavelength dye laser pumping the relative fraction of the probe beam converted to the signal beam varied quadratically with laser power for all conditions investigated. Pumping with the higher power argon-ion laser at shorter wavelengths also produced quadratic dependences of FWM signal efficiencies at high write-beam crossing angles, but saturation effects were observed for small crossing angles as seen in Fig. 4. If the write beams are oriented to cross near the surface of the sample, significant deviations from quadratic behavior and saturation effects are observed.

### III. DISCUSSION AND CONCLUSIONS

These results can be interpreted in terms of the model of FWM (Refs. 12 and 13) based on scattering from a laser-induced, transient population grating. The interference of the Gaussian wave fronts of the write beams in the region of their crossing forms a sinusoidal pattern resulting in a similar spatial distribution of  $\text{Cr}^{3+}$  ions in the excited state. Because of the difference in the absolute

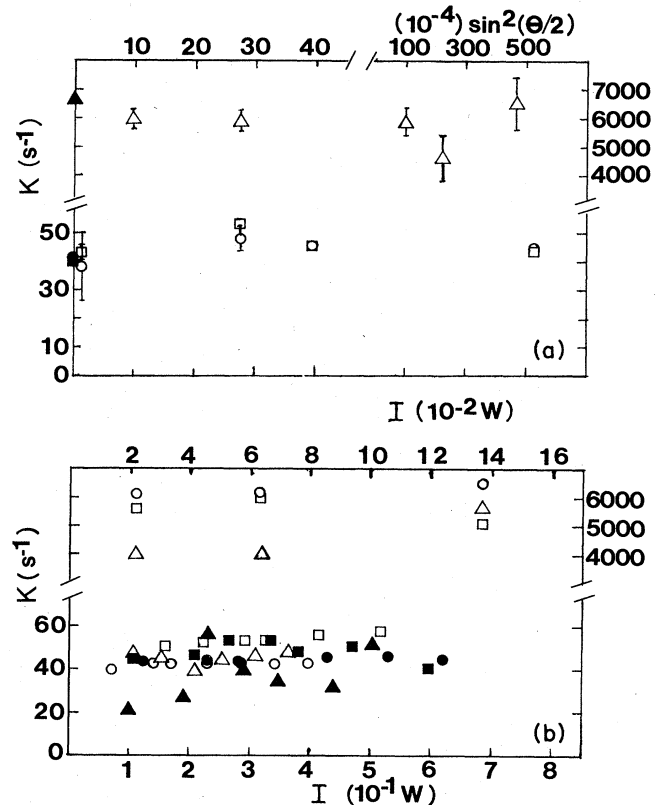


FIG. 3. (a) FWM signal decay rate versus pump beam crossing angle:  $\lambda_x=579.1$  nm ( $\Delta$ );  $488.0$  nm ( $\circ$ ); and  $514.5$  nm ( $\square$ ). The solid points represent twice the fluorescence decay rates. (b) FWM signal-decay rate versus total pump beam power. Upper scale for  $\lambda_x=579.1$  nm:  $\theta=3.5^\circ$  ( $\circ$ );  $\theta=11.5^\circ$  ( $\Delta$ );  $\theta=17.3^\circ$  ( $\square$ ). Lower scale for  $\lambda_x=488.0$  nm:  $\theta=1.75^\circ$  ( $\blacktriangle$ );  $\theta=6.0^\circ$  ( $\blacksquare$ );  $\theta=26.5^\circ$  ( $\bullet$ ); and for  $\lambda_x=514.5$  nm:  $\theta=1.75^\circ$  ( $\triangle$ );  $\theta=6.0^\circ$  ( $\square$ );  $\theta=26.5^\circ$  ( $\circ$ ).

value of the complex dielectric constant of the material when the  $\text{Cr}^{3+}$  ions are in the ground or excited states, this sinusoidal excited-state population distribution acts as a diffraction grating which scatters the read beam. When the Bragg condition is satisfied, this becomes the FWM signal beam which can be theoretically expressed as<sup>4</sup>

$$\eta(t) \propto [\Delta N(I)]^2 = \eta_p e^{-Kt}, \quad (1)$$

where  $\Delta N$  is the difference in the concentration of excited  $\text{Cr}^{3+}$  ions between the peak and valley regions of the grating and  $I$  is the power of the laser write beams. The decay rate  $K$  contains terms describing all physical processes contributing to the grating relaxation. The term related to the fluorescence decay of the excited ions is  $2/\tau$ , where  $\tau$  is the fluorescence decay time of the ions in the excited state. Other terms depend on  $\theta$  (such as long-range energy migration) or on laser power (such as stimulated emission). The fact that the results obtained here exhibit exponential decays with  $K=2/\tau$  independent of  $\theta$  and  $I$  shows that the gratings created are excited-state-population gratings and that no effects of long-range ener-

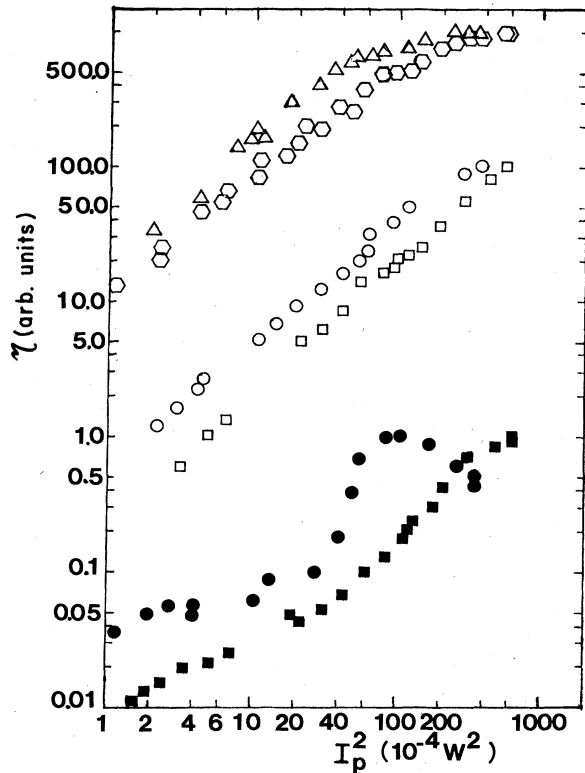


FIG. 4. Fraction of probe beam converted to FWM signal beam as a function of the product of the powers of the laser pump beams. Bulk:  $\lambda=488.0$  nm,  $\theta=6^\circ$  (O);  $\lambda=514.5$  nm,  $\theta=6^\circ$  ( $\Delta$ );  $\lambda=488.0$  nm,  $\theta=26.5^\circ$  ( $\square$ );  $\lambda=514.5$  nm,  $\theta=26.5^\circ$  ( $\circ$ ). Surface:  $\lambda=488.0$  nm,  $\theta=26.5^\circ$  ( $\blacksquare$ );  $\lambda=514.5$  nm,  $\theta=26.5^\circ$  ( $\bullet$ ).

gy transfer or stimulated emission are contributing to the grating decay.

The fact that the decay rates are significantly different for the two different types of laser excitation can be understood from the absorption and fluorescence spectra shown in Fig. 5. The dye laser excitation at 579.1 nm efficiently excites  $\text{Cr}^{3+}$  ions in the mirror sites as demonstrated by the dominance of the two  $R_m$  lines in the fluorescence spectrum. The measured fluorescence decay rate is consistent with that of the coupled emission from the  ${}^2E$  and  ${}^4T_2$  levels of  $\text{Cr}^{3+}$  ions in this type of site.<sup>2</sup> On the other hand, the 488.0- and 514.5-nm excitation wavelengths of the argon laser excite a significant number of  $\text{Cr}^{3+}$  ions in the inversion sites as seen by the enhancement of the  $R_i$  lines from these sites in the fluorescence spectrum. The smaller fluorescence decay rate is consistent with the weaker transition strengths of ions in this type of site.<sup>2</sup> Excitation spectra for the ions in the two types of sites verify the existence of different absorption bands associated with these ions which result in the selective excitation for the three different wavelengths used.<sup>14</sup>

The strength of the FWM signal depends on the difference of the concentration of ions in the excited state between the peak and valley regions of the grating  $\Delta N$  and on the difference in the complex dielectric constant of the

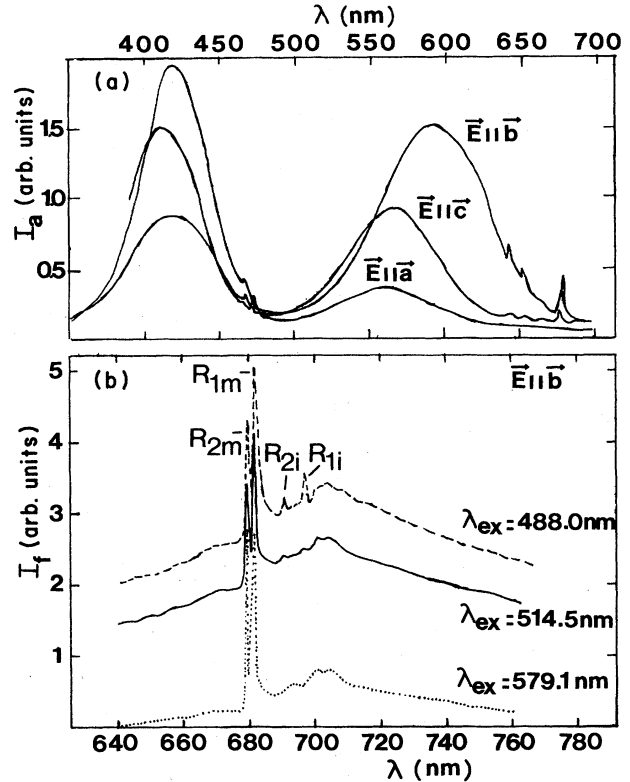


FIG. 5. Absorption and fluorescence spectra of  $\text{BeAl}_2\text{O}_4:\text{Cr}^{3+}$ .

material when the ions are in the excited state and when they are in the ground state. The former depends on the cross section of the  ${}^4A_2-{}^4T_2$  transition which is seen in Fig. 5(a) to be large for  $\vec{E}||\vec{b}$ , medium for  $\vec{E}||\vec{c}$ , and small for  $\vec{E}||\vec{a}$ . This is consistent with the fact that a strong FWM signal is only observed with the first of these polarization orientations, a weak signal with the second, and no signal with third.

The complex dielectric constant is  $\epsilon = \epsilon_r + i\epsilon_i$ . The change in  $\epsilon$  can be associated with either a difference in the absorption coefficient,  $\Delta\alpha = \frac{1}{2}(2\pi/\lambda)\Delta\epsilon_i/(\epsilon_i)^{1/2}$ , or a difference in the refractive index,  $\Delta n = \frac{1}{2}\Delta\epsilon_r/(\epsilon_r)^{1/2}$ . In a simple two-level model, the expression for FWM scattering efficiency is given by<sup>12</sup>

$$\eta = e^{-2\bar{\alpha}\Gamma} [\sinh^2(\Delta\alpha\Gamma/2) + \sin^2(\pi\Delta n\Gamma/\lambda)], \quad (2)$$

where  $\Gamma = d/\cos\theta$  with  $d$  being the sample thickness and  $\bar{\alpha}$  is the average absorption coefficient at the laser wavelength  $\lambda$ . Absorption gratings are associated with differences in the absorption cross sections of ions in the ground and excited states. The peak-to-valley difference in the absorption coefficient grating is<sup>15</sup>

$$2\Delta\alpha = \frac{2[N_0 I_0 \sigma_1 (\sigma_2 - \sigma_1)]}{2I_0 \sigma_1 + (h\nu)\tau_{21}^{-1}}, \quad (3)$$

where  $N_0$  is the total concentration of active ions,  $I_0$  is the energy density of the laser pump beams with photon

energy ( $h\nu$ ), and  $\tau_{21}$  is the fluorescence decay time of the excited state.

Under optimum conditions, the scattering efficiency is measured to be approximately  $10^{-3}$ . Using Eq. (3) and the excited-state absorption results reported in Ref. 8, the numerator in Eq. (2), which represents the contribution to the scattering due to an absorption grating, can be calculated. Then using this result and the measured value for  $\eta$  in Eq. (2), the denominator, which represents the contribution to the scattering due to a dispersion grating, can be estimated. For the three laser pump wavelengths used in this work, the ratios of the absorption grating term to the dispersion grating term are  $3.0 \times 10^{-4}$  (488.0 nm),  $0.0$  (514.5 nm), and  $3.0 \times 10^{-6}$  (579.1 nm). These results indicate that for these excitation wavelengths the FWM signal is due mainly to scattering from a dispersion grating. The parameters obtained from this work are summarized in Table I.

It is difficult to theoretically calculate the contribution to the FWM signal due to dispersion changes since this involves the sum over all possible transitions of the  $\text{Cr}^{3+}$  ions in both the ground and metastable states. Using a simple two-oscillator model for dispersion, the change in the index of refraction between the peak and valley regions of the grating can be approximated as<sup>16</sup>

$$2\Delta n = (N_{2p}/n_0) \{ f'_1 (1 - \omega/\omega_1) / [4(\omega_1 - \omega)^2 + \gamma_1^2] + f'_2 (1 - \omega/\omega_2) / [4(\omega_2 - \omega)^2 + \gamma_2^2] \}. \quad (4)$$

Here  $f'_i$  is the effective oscillator strength of the  $i$ th transition,  $\gamma_i$  is the width of the transition, and  $\omega_i - \omega$  is the detuning from the center of the transition.  $n_0$  is the index of refraction of the unperturbed sample.  $N_{2p}$  represents the number of ions in the excited state in the peak region of the grating which is given by

$$N_{2p} = 2I_0 N_0 \sigma_1 / [2I_0 \sigma_1 + (hc/\lambda\tau_{21})]. \quad (5)$$

Taking the two transitions originating from the ground and metastable states closest to resonance with the incident laser frequency, Eqs. (4) and (5) predict values of  $\Delta n$  three orders of magnitude smaller than those listed in Table I. The required values of  $\Delta n$  can be obtained from this simple model only if the high oscillator strength charge-transfer transitions in the near uv spectral region are included. This latter conclusion is important in developing a general understanding of the FWM signal in materials such as transition-metal and rare-earth-doped crystals.

The fact that saturation of the scattering efficiency versus power occurs at small pump beam crossing angles and not at large angles may be due to the efficiency of coupling the light laser power level in Fig. 4, the effective

TABLE I. Summary of results of FWM measurements on alexandrite.

Parameter	Excitation wavelength (nm)		
	488.0	514.5	579.1
$\eta$	$\sim 10^{-3}$	$\sim 10^{-3}$	$\sim 10^{-3}$
$I_0$ (W/cm <sup>2</sup> )	60	60	12
$\lambda_{21}$ (ms)	49.1	50.3	0.30
$\bar{\alpha}$ (cm <sup>-1</sup> )	0.36	0.54	2.80
$N_{2p}$ (cm <sup>-3</sup> )	$8.74 \times 10^{17}$	$1.31 \times 10^{18}$	$5.3 \times 10^{16}$
$\Delta\alpha$ (cm <sup>-1</sup> )	$2.62 \times 10^{-3}$	0.00	$-8.70 \times 10^{-4}$
$\Delta n$	$6.74 \times 10^{-5}$	$7.78 \times 10^{-5}$	$2.72 \times 10^{-4}$

power inside the sample is significantly greater for the  $\theta = 6^\circ$  data than for the  $\theta = 26.5^\circ$  data. The values of  $N_{2p}$  listed in Table I for the three excitation wavelengths represent 13% (488.0 nm), 19% (514.5 nm), and 0.22% (579.1 nm) of the ions available. Thus a significant number of  $\text{Cr}^{3+}$  ions are in the  ${}^2E$  level in these experiments but the total saturation level of 50% is not reached. Note that Eq. (5) shows that  $N_{2p}$  depends on the absorption cross section, the laser power, and the metastable-state lifetime. For  $\text{Cr}^{3+}$  ions in the inversion sites the first of these factors is small but the latter two are large compared to the ions in the mirror sites. This explains why  $N_{2p}$  can be large for pumping with argon laser wavelengths which fall in the valley between the two major absorption bands shown in Fig. 5.

The FWM signal efficiency for alexandrite is approximately the same as that of a similar sample of ruby. FWM in ruby has been investigated by several workers<sup>13,15,17-19</sup> and the signal has been attributed to a  $\text{Cr}^{3+}$  population grating as proposed here. There is some disagreement as to whether scattering is due to an absorption or dispersion grating. Thermal gratings with shorter, angle-dependent decay rates were also observed in ruby<sup>19</sup> and will be the subject of a future investigation of alexandrite. For both ruby and alexandrite crystals the laser-induced changes in the dielectric constant are significantly greater for the population gratings created through pumping the  $\text{Cr}^{3+}$  ions than for intrinsic host-crystal properties investigated by off-resonance pumping.<sup>20</sup> The nonlinear properties of the type investigated here are known to affect laser operational properties in ruby<sup>21</sup> and thus may also be important in alexandrite laser operation.

#### ACKNOWLEDGMENTS

This work was sponsored by grants from Allied Chemical Corporation, the U.S. Army Research Office, and the National Science Foundation under Grant No. DMR 82-16551.

<sup>1</sup>J. C. Walling, *Laser Focus* 18, 45 (1982).

<sup>2</sup>J. C. Walling, O. G. Peterson, H. P. Jenssen, R. C. Morris, and E. W. O'Dell, *IEEE J. Quant. Elect.* **QE-16**, 1302 (1980).

<sup>3</sup>J. C. Walling, H. P. Jenssen, R. C. Morris, E. W. O'Dell, and O. G. Peterson, *Opt. Lett.* **4**, 182 (1979).

<sup>4</sup>J. C. Walling and L. Horowitz, in *Lasers 80*, edited by C. B. Collins (STS, McLean, Virginia, 1980), p. 534.

<sup>5</sup>J. C. Walling and O. G. Peterson, *IEEE J. Quant. Elect.* **QE-16**, 119 (1980).

<sup>6</sup>C. F. Cline, R. C. Morris, M. Dutoit, and P. J. Harget, *J.*

- Mater. Sci. **14**, 941 (1979).
- <sup>7</sup>M. L. Shand, J. Appl. Phys. **54**, 2602 (1983).
- <sup>8</sup>M. L. Shand, J. C. Walling, and R. C. Morris, J. Appl. Phys. **52**, 953 (1981).
- <sup>9</sup>B. K. Sevast'yanov, Yu. I. Remigailo, V. P. Orekhova, V. P. Matrosov, E. G. Tsvetkov, and G. V. Bukin, Dokl. Akad. Nauk SSR **256**, 373 (1981) [Sov. Phys.—Dokl. **26**, 62 (1981)].
- <sup>10</sup>J. Feinberg, in *Optical Phase Conjugation*, edited by R. A. Fisher (Academic, New York, 1983), p. 417.
- <sup>11</sup>C. M. Lawson, R. C. Powell, and W. K. Zwickler, Phys. Rev. B **26**, 4836 (1982); Phys. Rev. Lett. **46**, 1020 (1981); and J. K. Tyminski, R. C. Powell, and W. K. Zwickler, Phys. Rev. B **29**, 6074 (1984).
- <sup>12</sup>H. Kogelnik, Bell Syst. Tech. J. **48**, 2909 (1969).
- <sup>13</sup>H. J. Eichler, J. Eichler, J. Knof, and Ch. Noack, Phys. Status Solidi A **52**, 481 (1979).
- <sup>14</sup>L. Xi, X. Gang, R. C. Powell, and J. C. Walling, (unpublished).
- <sup>15</sup>K. O. Hill, Appl. Opt. **10**, 1695 (1971).
- <sup>16</sup>K. A. Nelson, R. Cassalegno, R. J. D. Miller, and M. D. Fayer, J. Chem. Phys. **77**, 1144 (1982).
- <sup>17</sup>D. S. Hamilton, D. Heiman, J. Feinberg, and R. W. Hellwarth, Opt. Lett. **4**, 124 (1979).
- <sup>18</sup>P. F. Liao, L. M. Humphrey, D. M. Bloom, and S. Geschwind, Phys. Rev. B **20**, 4145 (1979); P. F. Liao and D. M. Bloom, Opt. Lett. **3**, 4 (1978).
- <sup>19</sup>H. Eichler, G. Salje, and H. Stahl, J. Appl. Phys. **44**, 5383 (1973).
- <sup>20</sup>M. J. Weber, D. Milam, and W. L. Smith, Opt. Eng. **17**, 463 (1978).
- <sup>21</sup>H. Eichler, P. Glozbach, and B. Kluzowski, Z. Angew. Phys. **28**, 303 (1970).